A dynamical analysis of oscillatory responses in the optic tectum

Sergio Neuenschwander [a], Jacques Martinerie [b], Bernard Renault [b] and Francisco J. Varela [a]

[a] *Institute of Neuroscience, CNRS, University of Paris 6, Paris (France) and* [b] *LENA, Hôpital de la Salpétrière, CNRS, University of Paris 6, Paris (France)*

Multi-unit recordings from the optic tectum of an awake pigeon displaying oscillatory behavior evoked by visual stimulus are highly non-stationary and contain a broad band of frequencies under a time-window analysis. Here we extend these observations by a non-linear dynamical analysis of these oscillatory signals (local fields potentials) in successive epochs during background activity and visual responses. Two numerical estimates have been obtained from the original data every 200 ms: (1) correlation dimension and (2) non-linear forecasting of the trajectories. Results from eight different recording sites analyzed are consistent and indicate, in the average, an increase in complexity of the signal during the oscillatory periods.

INTRODUCTION

The hypothesis that neuronal synchronization can provide a mechanism to integrate the activity of the neurons underlying a perceptual task has received a fair amount of attention recently (see ref. 8 for review). The interest stems from the recognized need to account for cognitive processes by the activity of a coherent population of cells, a neuronal ensemble, and not by the isolated observation of single neuronal responses[1,10,34]. In these studies, cell assemblies are viewed as dynamical entities that arise from a transitory phase-locking of activity between their elements, binding distinct regions in the brain.

The biological reality of the synchronization mechanism was first suggested by behavioral studies of olfactory discrimination in the rabbit, where macro potentials showed coherent oscillations in response to motivation and learning[10,11]. More recently, synchronized responses (multi-unit activity) have been demonstrated in other structures, most extensively in the visual cortex of lightly anesthetized cats[6,7,14,15], but also in the visual and somatosensory cortex of monkeys[19,20,23], and in the

avian optic tectum[24–26]. In all these studies, neurons tend to assume a structured firing in response to visual stimuli, seen in recurrent bursts of spikes, correlated with the local field potential, both showing marked oscillations in the gamma band, around 30–70 Hz. These oscillations seem to be the support for the synchronization process, as has been shown explicitly in the cat's visual cortex by means of multi-unit recordings in distant sites[8,25].

In all cases studied, these oscillatory episodes are far from stationary, as they have a limited duration of a few hundred milliseconds. Non-stationary episodes have been revealed by a moving window analysis over a single response epoch in awake monkeys and pigeons[19,26] and in the lighly anesthetized cat[14,16]. The oscillations also contain a substantial amount of jitter, with frequencies distributed over a broad spectrum. In view of these results, an important element missing in this field of study is a quantitative analysis of the dynamics of this transient characteristic of the signals associated with the phase-coupling of distributed oscillators. Theoretical studies proposing neural models capable of engendering synchronization through oscil-

---

Correspondence: F.J. Varela, Institute of Neuroscience, 9 Quai St. Bernard, 75005 Paris, France.

latory behavior, have assumed that neuronal synchronization is a resonance-type process, reducing a largely incoherent background activity into a limited cycle with a narrow spectrum in the gamma range (e.g. see ref. 18). However, this is unlikely to be the case given the complexity of the physiological and anatomical constitution of the neuronal populations involved. Experimentally, the oscillations are non-stationary and broadly distributed, as mentioned before[26,16].

The purpose of this paper is to report on some measures of the dynamical behavior of the local field potential recorded from the avian optic tectum in awake pigeons, as a first step to address the issues raised above. Our analysis has been performed on sliding windows over single sweeps of the local field potential (LFP), that is, the electrical activity of a local group of neurons recorded from a microelectrode, and filtered between 1–100 Hz, including background activity and responses to a moving bar. The techniques that have been applied to oscillatory signals so far have been essentially based on classical estimates of spectra and autocorrelation methods[26]. These procedures remain important but do not do full justice to the dynamics of the data. Applications of non-linear dynamics[5] to brain signals are likely to be useful for understanding complex physiological phenomena (for a collection of representative papers see refs. 3 and 4). More specifically, assuming that some set of measured brain activity can be modeled by a dynamical system on a n-dimensional manifold M, the problem is that of reconstructing the trajectory of the system in its phase space without knowing the state variables. The only available information about the dynamics is from measurements given by a uni-dimensional time series. In our case, the time series is the LFP.

In the theoretical case of infinite and non-noisy time series, it has been demonstrated[33] that M can be embedded in R^{2n+1}. In the practical, non-ideal case, the following problems must be addressed: (1) what is the minimum number of variables n represented by the dimension of the system's attractor; (2) what is the nature of the system's state: stable, periodic, chaotic or random, during different phases of the resting activity or visual response. To answer these questions, two numerical estimates are useful in order to quantify some aspects of the dynamic structure and the evolution of the system trajectories: (1) the correlation dimension which is a static index representing the density of points in the state space, and which is related to the number of degrees of freedom of the system; (2) the local non-linear forecasting[32] which characterizes the divergence of the neighboring trajectories and is related to the largest Liapunov exponent of the system.

Using these methods, we show here that, perhaps contrary to intuition, the complexity of the signal increases during the oscillatory periods.

MATERIALS AND METHODS

Electrophysiological recordings

The full details for the collection of the data reported here has been described elsewhere[26]. In brief, a head bolt and recording chamber were first surgically implanted onto the skull of adult pigeons under anesthesia to provide free access to the optic tectum. Recording sessions were performed with the awake animal having its head fixed and its gaze directed to a tangent screen. The visual stimuli consisted in a projected light bar swept onto the receptive field. Single glass-coated tungsten electrodes (0.5–1.0 MΩ impedance) were used to record tectal units. The single trials had a duration of 2 s, and included responses to the forward and backward movement of the stimulus.

Data collected from the tectum were amplified 1000×, and a local field potential obtained by digitally filtering at 1–100 Hz. The LFP was recorded with 5 kHz sampling rate by means of a 12 bit converter. In addition, multi-unit activity was recorded after filtering the compound signal at 0.5–3 kHz, and counting the spike events by an amplitude threshold trigger. The oscillatory behavior of the LFP was estimated by autocorrelation methods: the autocorrelation function of the LFP was computed in 200 ms windows moved over single sweeps in steps of 100 ms. A Gabor function was fitted to the autocorrelograms and their parameters used to estimate the degree of significance of the oscillatory activity, following closely the criteria proposed by Engel et al.[7] for the cat. Basically an oscillation was considered significant if the decay of the Gabor function over its period (τ/T) was greater than 1.0.

Numerical analysis

State space reconstruction

In general, there is no unique way to construct a multi-dimensional phase space from experimental data. Instead, one uses the embedding theorems of Whitney[35] and Takens[33] to build up the phase space matrix of the attractor from a time series $X(t_i) = \{X(t_i), X(t_i + \theta), X(t_i + 2\theta), ... X(t_i + (M-1)\theta)\}$, topologically equivalent to the original set of variables and obtained by shifting the time series by a fixed time lag θ equal to the first minimum of the mutual information, which is a convenient tool to detect moments of minimum predictability in a time series[9]. Next a matrix is constructed from the components of the vectors $X(t_i)$, and a singular value decomposition (SVD) is performed[2], which is a standard noise reduction technique that is related to principal component analysis, changing the coordinate system to provide an optimal representation of the trajectory of the system. If the eigenvalues are less than a threshold value (10^{-4}) the axis is discarded, one can thus work in a smaller dimensional space than the original one (see Methods in ref. 28). In practice, time series are neither infinite nor noise-free, and cause this method to yield results that are highly dependent on the size of the data window used for analysis. None of the methods used so far to determine the value of the window size give an optimal estimate[21]; our choice here was guided by empirical constraints of the experimental analysis (see below).

Correlation dimension

The evaluation of dimension (or correlation exponent, D_2) is performed by the Grassberger–Proccacia algorithm[12,13]. It should be noted that this estimate does not measure the topological dimension of the phase space in which the trajectories of the attractors evolve. Rather, it quantifies how much portion of this phase space is occupied by the attractor. In general this correlation exponent is a fractal number (non-integer). The technical difficulties that are encountered using this algorithm with sets of noisy data should not be
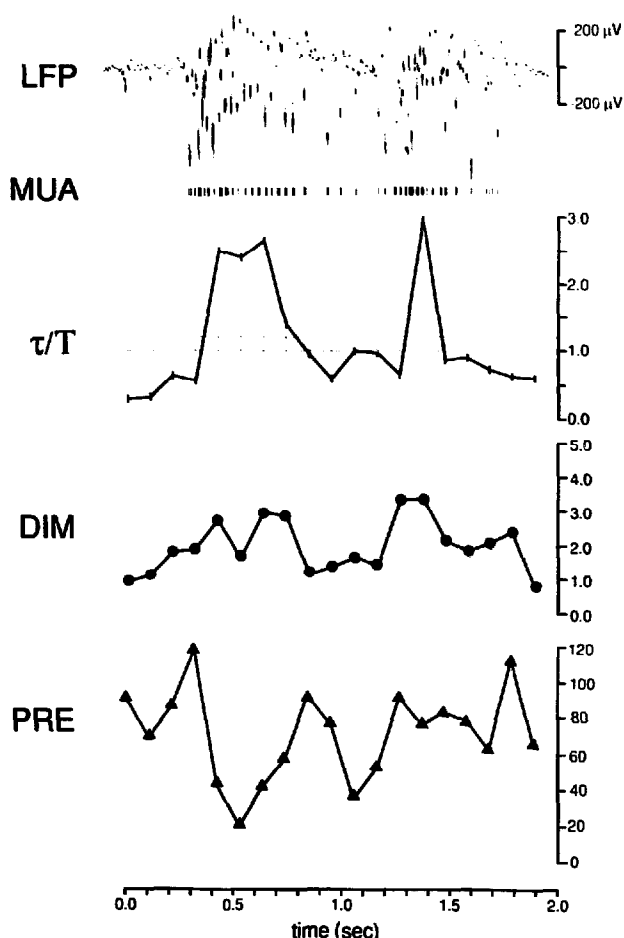
Fig. 1. Data from a multi-unit recording from the pigeon optic tectum (recording site D, trial 1), displaying the local field potential (LFP), and the corresponding bursts of spikes (MUA). The significant oscillatory epochs (see Materials and Methods) are indicated by a square, in 200 ms windows, together with the steepness of the fitted Gabor function (τ/T), a measure of the presence of an oscillation. Below, the correlation dimension D_2 (DIM) and the non-linear forecasting (PRE) of the reponse computed in succesive 2C0 ms windows.

underestimated. It is possible to impose conditions on the calculation that reduce the possibility of spurious estimates, but noisy experimental data can fail to satisfy these criteria[21]. To test the algorithm, we obtained the expected values for the D_2 of the Rössler and
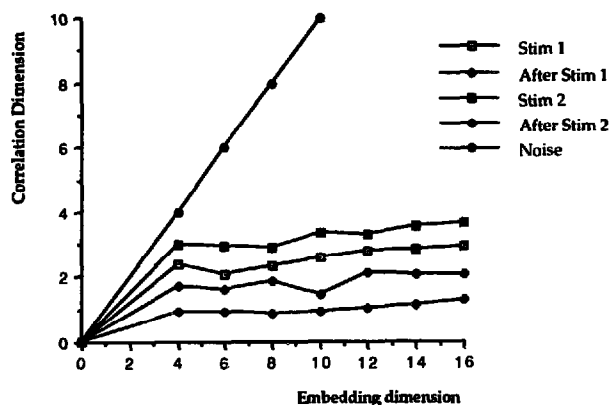
Lorenz attractors, and of standard periodic functions (one, two, and three sine waves related with irrational ratios in their frequencies and of the same amplitude).

Another technical point of significance here is that the choice of the time-window for dynamical analysis is more important than the number of vectors selected. Small size time-windows should be preferred to non-stationary dynamical systems. In our study in the pigeon, we used a 200 ms time-window since it corresponded to the average duration of the oscillatory phenomena under study[26]. Accordingly, we have used the same time-window for our calculations here; increasing the window size to 300 ms or more only leads to a smoothing of the results. For small data sets 10% of the total of variance is due to the use of small numbers of vectors (less than 400) while 90% comes from variations due to window size used[17]. However, the number of vectors used is also an important consideration, since a large number of vectors can lead to an underestimation of the complexity measure. We have used a modified version of the Grassberger–Proccacia (see below) using 1000 vectors as a good compromise for avoiding underestimation of D_2. In practice, the maximum value (D_2 max) is related to the number N of time series as follows: D_2 max ≤ 2 log N^{29}. Since in our study $N = 1000$, we should not retain dimensions greater than 6.

Our electrophysiological study of LFP signals requires a high sampling rate (to preserve the spike data) yielding 1000 vectors for the calculation in each 200 ms time-window chosen. For these conditions, we have modified the Grassberger–Procaccia algorithm as follows: the pair X_i, X_j was excluded from computation if $|i-j| > \theta$, where θ is the first minimum of mutual information. Besides, if the length of the plateau or of the scaling region was less than 12 points the dimension estimate was rejected. The dimension of D_2 as a function of embedding dimension must be stable and determine a good saturation which is considered as a necessary condition. The estimate of the (saturated) correlation dimension was calculated for each of the 200 ms data windows (1000 time shifted vectors) along the 2 s trials on a maximun of 16 embedding dimensions. The required CPU time on a DEC MicroVax 3100 computer was about 12 h for each recording site analyzed.

Non-linear local forecasting

The basic idea that deterministic laws govern a system even if it is non-linear or even chaotic, makes it possible that the future may be predicted for short time periods from the past behavior. We have computed an index of the evolution of the neighboring trajectories using the Sugihara and May[32] method, which consists of computing the linear correlation between the observed trajectory and a predicted one. In other words, this method uses a local linear estimate in order to produce a global non-linear predictor. The prediction is made using the first half of the signal (after SVD in our case) as a learning set of the evolution of its neighborhoods in the signal's phase space. The space is divided into subspaces by the median on each axis (k-tree method) to speed up the procedure. The index thus obtained gives a system's 'signature' for a short-time extrapolation

Fig. 2. Convergence plateaus for the estimation of the embedding dimension. Data for recording site D, trial 1.

TABLE I

Correlation dimension

Recording site	Trial number	Initial state	Stimulus 1	After stimulus 1	Stimulus 2	After stimulus 2
C	1	2.40	2.94	0.92	3.62	2.39
C	9	2.23	3.13	1.85	4.22	1.98
D	1	1.30	2.42	1.42	2.96	1.76
D	2	3.60	2.42	1.01	2.92	1.80
D	3	2.50	2.83	1.21	3.05	1.55
B	2	1.95	4.13	2.00	3.14	2.81
A	2	3.66	4.49	4.04	3.75	2.47
E	8	3.08	5.03	3.38	5.04	1.85
Mean		2.59	3.42	1.98	3.58	2.08
S.E.		0.28	0.35	0.44	0.26	0.15

TABLE II

Predictability index

Recording site	Trial number	Initial state	Stimu- lus 1	After stimu- lus 1	Stimu- lus 2	After stimu- lus 2
C	1	113	79.8	85.3	77.8	76.3
C	9	88.5	70	107.6	62.3	62.8
D	1	83.4	56.8	64.8	84.4	80
D	2	90.3	57.4	91.8	63	109.4
D	3	83.7	58.3	60.2	58.8	114.7
B	2	79.5	89.8	77.9	82.3	85.5
A	2	110.5	109	112.2	75.8	87
E	8	87.7	76.7	111	99.8	86.3
Mean		92.1	74.72	88.85	75.52	87.75
S.E.		4.47	6.47	7.23	4.87	6.00

TABLE III

Average τ/T

	Initiale state	Stimu- lus 1	After stimu- lus 1	Stimu- lus 2	After stimu- lus 2
Mean	0.34	0.77	0.49	0.76	0.50
S.E.	0.03	0.12	0.05	0.12	0.006

(10 prediction time points). The signature of a chaotic process is that the correlation decreases as the prediction time increases, while in random and periodic processes there is a constant and time-independent correlation. For periodic systems the magnitude of this correlation coefficient is related to the signal/noise ratio, and is equal to 1 for a pure sine wave, while for a random signal the constant is near 0. To characterize the signature along the 10 prediction time points selected, we have computed the linear slope of the curve joining these values, in order to study its evolution along the entire 2 s of the raw data. Accordingly, a decrease in value of this parameter indicates the emergence of an oscillatory period.

RESULTS

Eight LFP signals (single trials) from 5 different recording sites (e.g. 19 windows analyzed for each trial, making a total 152 time series) have been studied with the methods described above and compared with the standard analysis (spectral power and autocorrelation) reported previously[26]. An example of data and analysis is shown in Fig. 1 displaying a 2 s raster of spike responses (MUA) and the corresponding LFP from a multi-unit recording (from a single electrode) in the pigeon optic tectum. The 200 ms windows during which there was a significant oscillation of the LFP (see Materials and Methods) are indicated by a rectangle of the window's duration, along with the τ/T ratio which characterizes the steepness of the autocorrelation function. It is seen that the forward and backward passage of the stimulus entrains a burst of spikes, an increase in the oscillatory appearance of the LFP, as well as the appearance of significantly oscillatory windows accompanied by an increase of the τ/T ratio.

We now consider how this standard analysis compares with the two dynamical measures studied here. These are indicated in the lower part of Fig. 1 in the same time scale, for ease of comparison. The value of

the correlation dimension (labelled as DIM) follows a pattern of decrease and increase in successive windows, specially in the later part of the sweep. For instance, the average value corresponding to the time between forward and backward stimuli is 1.42, increasing to 2.96 for the backward stimulation. These are reliable numerical estimates since they were obtained from the curves for increasing embedding dimensions displaying important plateaus (or scaling regions), as illustrated in Fig. 2. That the pattern just discussed for the data of Fig. 1 is a representative one can be seen by taking averages over all the different recording sites and trials studied (Table I). On the average there is a significant increase when the values during stimulations are compared with those during background activity (i.e. no stimulus present) (Manova, $F_{1,7} = 46.52$, $P = 0.0002$). Thus the oscillatory periods are characterized by a more than one additional dimension of complexity than the inter-stimulus segments.

The index for local forecasting appears to follow the inverse pattern than that of correlation dimension. For example, in Fig. 1 the prediction index displays the signature of a rather chaotic activity (with an average of 83.4 for the first 300 ms), becoming quasi-periodic during the forward movement between 400–700 ms (56.8 on the average). A similar sequence of increase and decrease is seen in the backward movement of the stimulus. Thus the predictability index indicates the emergence of a pseudo-periodic activity during oscillatory periods, but one which is far from a pure frequency which should display a null slope. This impression is confirmed by calculating the same averages as those obtained for the correlation dimensions (Table II). The differences in this case also reach significant levels when the periods with visual stimulation vs. background activity are compared (Manova, $F_{1,7} = 9.32$, $P = 0.018$). Notice that there is an apparent shift of about 100 ms in the stimuli-related changes of both dynamical measures just discussed. This as an epiphenomenon due to the fact that for computing the pre-
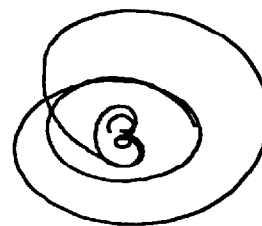
Fig. 3. Trajectories from the first two and most significant axes (see Materials and Methods) of the trajectories from recording site C, trial 1 in succesive time-windows. The underlined times indicates epochs where the visual stimulus was present.
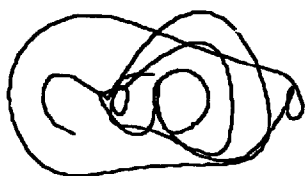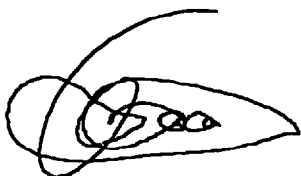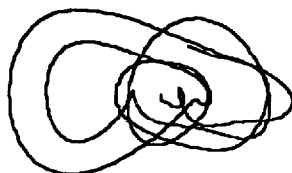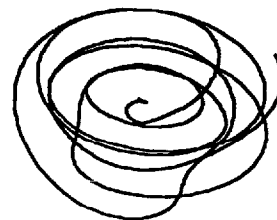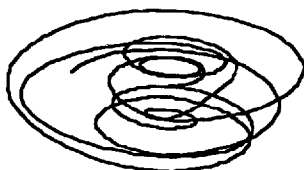
100   msec
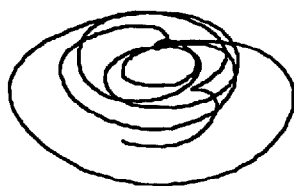
600

1100

200

700

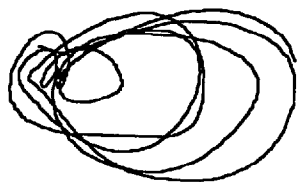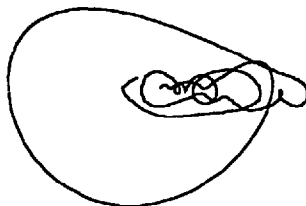**1200**

300
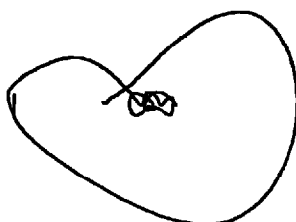
800
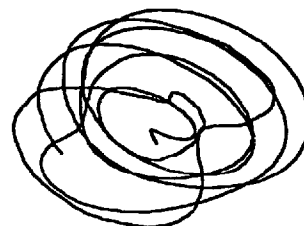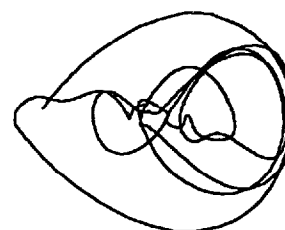
1300
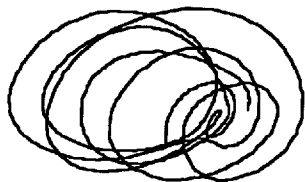
400
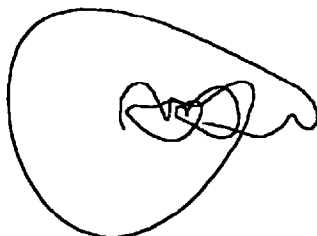
900
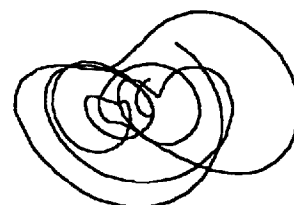
1400

500

1000

1500   msec

dictibility index we consider only the first half (100 ms) of the window of analysis so as to calculate the trajectories.

It is interesting to consider the relation between the presence of an oscillatory period and the two indices just described. As shown in Table III, the value of τ/T, which is a quantitative measure of the presence of a strong oscillation within the 200 ms window, increases significantly (Manova, $F_{1.7} = 12.43$, $P = 0.0097$) during the periods of visual stimulation. However, this clear correspondence is less apparent if one follows the individual time-windows for each recording site. More specifically, we found that only for half of the recording sites there was a postive correlation (Spearman–Rank correlation value of less than 0.39, $n = 18$ time-windows per recording site) between τ/T and D_2, or a negative correlation between τ/T and the prediction index PRE. Thus the ocurrence of oscillations is not always in a precise temporal correspondence with the indicators for complexity used here.

A plot of the trajectories along the two main inertial axes (i.e. the main components of the SVD; see Materials and Methods) of the signal permits a more vivid appreciation of the system's dynamics as shown in Fig. 3. In the initial windows, the activity is characterized by a complex trajectory which is nevertheless distinctly different from a random signal, and is better described as a chaotic state. This period is followed by a more rhythmic signal, as can be seen in the mixture of at least two circular trajectories. During the intertrial interval, the signal is simplified into what looks like a low frequency limit cycle, which is followed once again by a pseudo-rhythmic activity. During the backward stimulus, the mixure of two circular trajectories reappears; the final windows fall once again into a simpler pattern. Thus, we can distinguish in succesive epochs of analysis at least three different kinds of trajectories. If one compares these images with those from a sinusoidal signal with random modification of amplitude or phase, the trajectories obtained bear a resemblance to the patterns just described, suggesting that the pseudo-periodicity of the electrical signals could be produced by a combination of oscillatory activities which have a dispersion or jitter in their phase and amplitude.

DISCUSSION

It is cleary premature to draw extensive conclusions from this first study, but we wish to underline certain suggestive possibilities for further examination.

Our results confirm the notion that a dynamical analysis of brain events complements and extends what can be concluded from more classical methods. In fact, those methods permit one to draw only limited conclusions about the transient and broad spectra quality of the signals analyzed. In contrast, a window-by-window measurement of the correlation dimension and nonlinear forecasting sharply puts into evidence that, on the average, the oscillatory periods correspond to an increase in signal complexity. The interplay of these three measures over individual time-windows is far less straightforward, and needs to be studied further. In particular, it should be kept in mind that the use of τ/T to detect oscillations demands that the oscillatory period be not only of large amplitude but also of regular frequency. This may contribute to explain the relative temporal disjunction between D_2, prediction and τ/T reported here. From a more general point of view it should be kept in mind that these three indicators are, in fact, related distinct characteristics of the neural signal.

The increase in complexity can be tentatively interpreted as a recruitment of a population of neurons that is larger than that which gives rise to the electrical signal in the inter-stimulus periods. This recruitment, possibly by phase synchrony amongst neurons, would increase the complexity of the brain signal being recorded locally and thus the degrees of freedom of the underlying system, as indicated by D_2. It is thus possible that the difference between background and the transient synchronization during visual stimulation amounts to the difference between a localized and relatively weak coupling, in contrast to a more extensively distributed and tighter coupling of the neurons involved. In a preliminary study of oscillations in the cat's visual cortex, Pawelzik[27] reaches comparable conclusions. The mathematical studies of Mathews et al.[22] would also support this neurophysiological interpretation since it shows that in a large population of coupled oscillators with a broad frequency range, synchronization can cover an important segment of phase space, and that between disorganization and phase-locking there are transitional regions characterized by unstable chaotic regimes.

The present results and the above interpretation seem to go somewhat counter to the earlier suggestion by Freeman[30] that during an oscillatory phase the attractor in the olfactory bulb was closer to a limit cycle, and that the system bifurcates from a complex background attractor to a simpler limit cycle during discrimination of odors. However, Skinner et al.[31] report that the correlation dimensions of their signals increased by about 0.8 during the learning phase for the odors, while it decreased after the odors had became familiar. The reasons for the differences between

our results and those of Freeman might have two sources (excluding technical differences derived from electrode size). First, the olfactory system is an exceptionally regular neural tissue, and might follow different dynamics (given its ancient phylogentic origins), than those of the more recent structures (such as tectum and neocortex) which involve more intricate assemblies underlying a cognitive task[36]. Second, perhaps in our experiments the animals were in a state of activation comparable to the learning phase in the experiments of Skinner et al.[31]. Both these reasons may contribute to our results during passive and repetitive visual stimulations. Further research is clearly necessary to address these issues.

REFERENCES

1 Abeles, M. (Ed.), *Local Brain Circuits*, Springer, Berlin, 1982.
2 Albano, A., Muench, J., Schwaetz, C., Mees, A. and Rapp, P., Singular valued decomposition and the Grassberg–Procaccia algorithm, *Phys. Rev.*, 38 (1988) 3017–3026.
3 Basar, E. and Bullock, T. (Eds.), *Brain Dynam.*, Springer, Berlin, 1989.
4 Basar, E. (Ed.), *Chaos in Brain Function*, Springer, Berlin, 1990.
5 Eckmann, J.P. and Ruelle, D., Ergodic theory of the chaos and strange attractors, *Rev. Mod. Phys.*, 57 (1985) 617–638.
6 Eckhorn, R., Bauer, R., Jordan, W., Brosch, M., Kruse, W. and Reitboeck, H.J., Coherent oscillations: a mechanism of feature linking in the visual cortex?, *Biol. Cybern.*, 60 (1988) 121–130.
7 Engel, A., König, P., Gray, C. and Singer, W., Stimulus-dependent neuronal oscillations in cat visual cortex: inter-columnar interaction as determined by cross-correlation analysis, *Eur. J. Neurosci.*, 2 (1990) 588–606.
8 Engel, A., König, P., Kreiter, A., Schillen, T. and Singer, W., Temporal coding in the visual cortex: new vistas on the integration of the nervous system, *Trends Neurosci.*, 15 (1992) 218–226.
9 Fraser, A. and Swinney, H., Independent coordinates for strange attractors from mutual information, *Phys. Rev.*, 33 (1986) 1134–1140.
10 Freeman, W., *Mass Action in the Nervous System*, Academic Press, New York, 1975.
11 Freeman, W. In A. Gevins and A. Remond (Eds.), *Handbook of Electroencephalography and Clinical Neurophysiology*, Vol. 1, 1987, pp. 583–662.
12 Grassberger, P. and Procaccia, I., Measuring the strangeness of strange attractors, *Physica*, 9 (1983) 189–208.
13 Grassberger, P. and Procaccia, I., Characterization of strange attractors, *Phys. Rev. Lett.*, 50 (1983) 346–349.
14 Gray, C.M. and Singer, W., Stimulus-specific neuronal oscillations in orientation columns of cat visual cortex, *Proc. Natl. Acad. Sci. USA*, 86 (1989) 1689–1702.
15 Gray, C.M., König, P., Engel, A.K. and Singer, W., Stimulus-dependent neuronal oscillations in cat visual cortex: receptive field properties and feature dependence, *Eur. J. Neurosci.*, 2 (1990) 607–619.
16 Gray, C.M., Engel, A., König, P. and Singer, W., Synchronization of oscillatory neuronal responses in cat striate cortex: temporal properties, *Vis. Neurosci.*, 8 (1992) 337–347.
17 Havstad, J. and Ehlers, C., Attractor dimension of non-stationary dinamical systems from data sets, *Phys. Rev. A*, 39 (1989) 845–853.
18 König, P. and Schillen, T., Stimulus dependent assembly formation of scillatory responses. I. Synchronization, *Neural Comput.*, 3 (1991) 155–166
19 Kreiter, A.K. and Singer, W., Oscillatory neuronal responses in the visual cortex of the awake macaque monkey, *Eur. J. Neurosci.*, 4 (1992) 369–375
20 Livingstone, M.S., Visually-evoked oscillations in monkey striate cortex, *Soc. Neurosci. Abstr.*, 17 (1991) 73.3.
21 Martinerie, J., Albano, I., Mees, A. and Rapp, P., Mutual information, ..ange attractors and the optimal estimation of dimension, *Phys. Rev.*, 45 (1992) 7058–7064.
22 Matthews, P., Mirollo, R. and Strogatz, S., Dynamics of coupled nonlinear oscillators, *Physica D*, 52 (1991) 293–351.
23 Murphy, V.N. and Fetz, E.E., Synchronized 25–35 Hz oscillations in sensori motor cortex of awake monkeys, *Soc. Neurosci. Abstr.*, 17 (1991) 126.11
24 Neuenschwander, S. and Varela, F.J., Sensory-triggered oscillatory activity in the avian tectum, *Soc. Neurosci. Abstr.*, 16 (1990) 47.6.
25 Neuenschwander, S. and Varela, F.J., Synchronization of oscillatory responses in the avian optic tectum, *Soc. Neurosci. Abstr.*, 18 (1992) 213.
26 Neuenschwander, S. and Varela, F.J., Visually-triggered neuronal oscillations in birds: an autocorrelation study of tectal activity, *Eur. J. Neurosci*, in press.
27 Pawelzik, K., *Nichtlineare Dynamik und Hirnaktivität*, Doctoral Dissertation, Verlag Harri Deutsch, Frankfurt, 1990.
28 Rapp, P., Bashore, T., Martinerie, J., Albano, A., Zimmerman, I. and Mees, A., Dynamics of brain electrical activity, *Brain Topography*, 2 (1989) 99–118.
29 Ruelle, D., Deterministic chaos: the science and the fiction, *Proc. R. Soc. London Ser A*, 427 (1990) 241–248.
30 Skarda, C. and Freeman, W., How brains make chaos in order to make sense of the world, *Behav. Brain Sci.*, 10 (1987) 161–195.
31 Skinner, J., Martin, J., Landisman, C., Mommer, M., Fulton, K., Mitra, M., Burton, W. and Salzberg, B., Chaotic attractors in a model of neocortex: dimensionalities of olfactory bulb surface potentials are spatially uniform and event related. In E. Basar and T. Bullock (Eds.), *Brain Dynamics*, Springer, Berlin, 1989, pp. 158–173.
32 Sugihara, G. and May, R., Nonlinear forecasting as a way of distinguishing chaos, from measurement error in time series, *Nature*, 344 (1990) 734–742.
33 Takens, F., Detecting strange attractors in turbulence. In D.A. Rand and L.S. Young (Eds.), *Dynamical Systems and Turbulence*, Lecture Notes in Mathematics 898, Springer, Berlin, 1981, pp. 365–381.
34 von der Malsburg, C., A neural-coktail party processor, *Biol. Cybern*, 54 (1986) 29–40.
35 Whitney, H., Differentiable manifolds. *Ann. Math.*, 37 (1936) 645–680.
36 Zeki, S. and Shipp, S.A., The functional logic of the cortical connections, *Nature*, 335 (1988) 311–317.